lubricants

Article

In Silico Approaches for Some Sulfa Drugs as Eco-Friendly Corrosion Inhibitors of Iron in Aqueous Medium

Soukaina Alaoui Mrani [1,†], Nadia Arrousse [1,*], Rajesh Haldhar [2,†], Abdellatif Ait Lahcen [3], Aziz Amine [3], Taoufiq Saffaj [4], Seong-Cheol Kim [2,*] and Mustapha Taleb [1]

[1] Laboratory of Engineering, Organometallic, Molecular and Environmental (LIMMOME), Faculty of Science, Sidi Mohamed Ben Abdellah University, Fez 30000, Morocco; soukaina-_-alaoui@hotmail.com (S.A.M.); mustaphataleb62@yahoo.fr (M.T.)
[2] School of Chemical Engineering, Yeungnam University, Gyeongsan 38541, Korea; rajeshhaldhar.lpu@gmail.com
[3] Faculty of Sciences and Techniques, Hussan II University, Casablanca 20000, Morocco; mtnorurlhouda33@gmail.com (A.A.L.); mliyed1992@gmail.com (A.A.)
[4] Faculty of Sciences and Techniques, Sidi Mohamed Ben Abdellah University, Fez 30000, Morocco; toufic.saffaj@usmba.ac.ma
* Correspondence: nadiaarrousse@gmail.com (N.A.); sckim07@ynu.ac.kr (S.-C.K.)
† These authors contributed equally to this work.

Abstract: This paper addresses the prediction of the adsorption behavior as well as the inhibition capacity of non-toxic sulfonamide-based molecules, also called sulfa drugs, on the surface of mild steel. The study of the electronic structure was investigated through quantum chemical calculations using the density functional theory method (DFT) and the direct interaction of inhibitors with the iron (Fe) metal surface was predicted using the multiple probability Monte Carlo simulations (MC). Then, the examination of the solubility and the environmental toxicity was confirmed using a chemical database modeling environment website. It was shown that the presence of substituents containing heteroatoms able to release electrons consequently increased the electron density in the lowest unoccupied and highest occupied molecular orbitals (LUMO and HOMO), which allowed a good interaction between the inhibitors and the steel surface. The high values of E_{HOMO} imply an ability to donate electrons while the low values of E_{LUMO} are related to the ability to accept electrons thus allowing good adsorption of the inhibitor molecules on the steel surface. Molecular dynamics simulations revealed that all sulfonamide molecules adsorb flat on the metal surface conforming to the highly protective Fe (1 1 0) surface. The results obtained from the quantum chemistry and molecular dynamics studies are consistent and reveal that the order of effectiveness of the sulfonamide compounds is P7 > P5 > P6 > P1 > P2 > P3 > P4.

Keywords: sulfonamide derivatives; toxicity; solubility; DFT calculations; MC simulation

check for updates

Citation: Mrani, S.A.; Arrousse, N.; Haldhar, R.; Lahcen, A.A.; Amine, A.; Saffaj, T.; Kim, S.-C.; Taleb, M. In Silico Approaches for Some Sulfa Drugs as Eco-Friendly Corrosion Inhibitors of Iron in Aqueous Medium. *Lubricants* **2022**, *10*, 43. https://doi.org/10.3390/lubricants10030043

Received: 16 February 2022
Accepted: 12 March 2022
Published: 15 March 2022

1. Introduction

Carbon steel is the largest class of alloys used in a variety of sectors such as industry and construction [1–3]. Nowadays, the common practice for some processes, e.g., cleaning, descaling, and pickling, is to use acidic solutions, as a result, the subsequent disintegration of metals is inescapable. Organic inhibitors are commonly applied to prevent the degradation of these metals in corrosive environments. As the new directives concerning industrial discharges are becoming more and more strict in eco-friendly terms, the development of eco-compatible and biodegradable corrosion inhibitors is becoming an important issue. In this context, we aim to investigate the corrosion inhibition behavior of seven sulfonamide-based compounds. Sulfonamides, generally known as sulfa drugs, are antimicrobial agents used to treat bacterial infectious diseases, they have low cost and broad-spectrum antimicrobial activity and are directly soluble in the acidic medium due to their basic character [4]. Sulfonamide compounds have different functional adsorption centers that may be –NH_2, –SO_2–NH– groups, O and N heteroatoms, and aromatic rings. It has been reported that the most effective organic inhibitors are those bearing nitrogen (N), sulfur (S), or oxygen (O) atoms in their structures [5,6]. The protective behavior of this type of molecule is often associated with their physical and/or chemical adsorption on the metal interface [7].

The expansion in computing power and the development of increasingly powerful algorithms have contributed to the evolution of material modeling techniques at the atomic scale. It is now possible to accurately characterize the properties of many materials by applying methods based on the fundamental laws of quantum mechanics and electromagnetism. The use of quantum chemical methods, in particular density functional theory (DFT), allows a rapid and accurate determination of the electronic structure and various molecular properties such as polarizability and excitation energy to evaluate the effectiveness of inhibitors [8]. A lower energy gap (EHOMO–ELUMO) corresponds to a higher molecular reactivity, which increases the degree of adsorption on the surface and, consequently, the inhibition efficiency [9]. In addition, the determination of Fukui indices allows the evaluation of the most active sites for nucleophilic and electrophilic attacks [10]. To fully understand the molecule–metal interaction, a Monte Carlo simulation study of the direct interaction of inhibitors with the iron (Fe) surface was performed. The inhibitor was placed on the surface of Fe (1 1 0) to find a suitable configuration [11,12].

2. Materials and Methods

2.1. In Silico Methodologies for Ecological Noxiousness and Solubility of Sulfonamide Derivative Inhibitors

The water solvency and toxicity of the investigated inhibitors (Figure 1) were assessed utilizing a chemical database with the modeling environment website [13]. This approach is to help the fundamental stages for quantitative structure activity relationship (QSAR) modeling, a strategy used to assess toxicity across the physical attributes of molecular structure design has a place with two subsystems: the fundamental phases of trial and the modeling framework [14].

2.2. DFT Calculations

The DFT calculations were performed using the Gaussian 09 software package with Beck's 3–parameter hybrid exchange functional (B3) combined with Lee–Yang–Parr (B3LYP) with 6-31G diffused and polarized (d,p) basis set of orbital [15]. The effect of solvent (water) was included in all DFT computations using the integral equation formalism variant of the polarizable continuum (IEFCPM). The quantum chemical descriptors have been extracted from the following equations to predict the corrosion inhibition properties of the investigated sulfonamide molecules [16].

$$\Delta E_{gap}(eV) = E_{LUMO} - E_{HOMO} \tag{1}$$

$$\chi = \frac{1}{2}(E_{HOMO} + E_{LUMO}) \tag{2}$$

$$\eta = \frac{1}{2}(E_{HOMO} - E_{LUMO}) \tag{3}$$

$$\sigma = \frac{1}{\eta} \tag{4}$$

$$\Delta N = \frac{\chi_{Fe} - \chi_{inh}}{2[\eta_{Fe} + \eta_{inh}]} \tag{5}$$

where ΔE_{gap} refers to energy gap, χ, η and σ are the absolute electronegativities and the absolute hardness and softness, respectively, and finally, ΔN is the fraction of electron transferred.

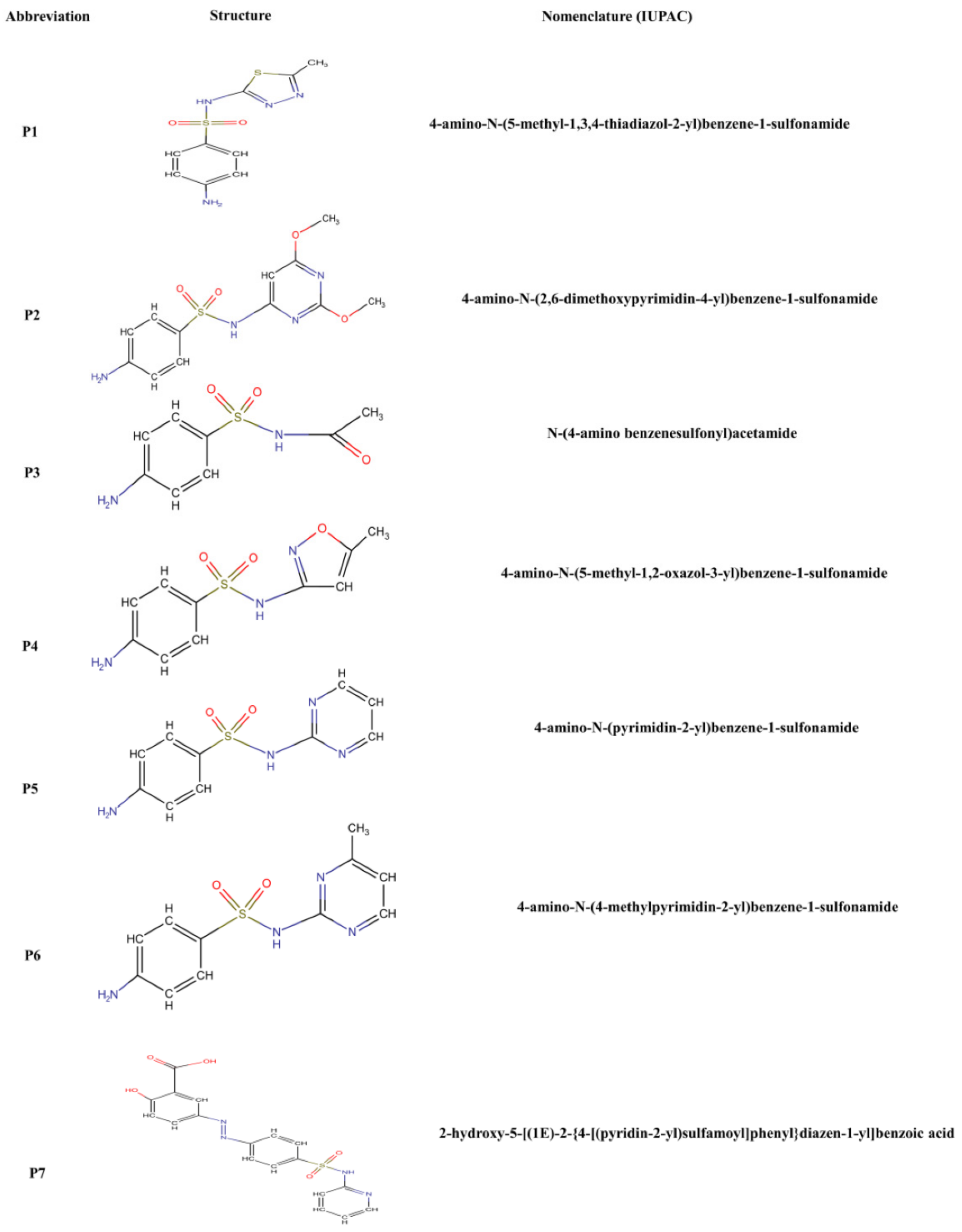

Abbreviation	Structure	Nomenclature (IUPAC)
P1		4-amino-N-(5-methyl-1,3,4-thiadiazol-2-yl)benzene-1-sulfonamide
P2		4-amino-N-(2,6-dimethoxypyrimidin-4-yl)benzene-1-sulfonamide
P3		N-(4-amino benzenesulfonyl)acetamide
P4		4-amino-N-(5-methyl-1,2-oxazol-3-yl)benzene-1-sulfonamide
P5		4-amino-N-(pyrimidin-2-yl)benzene-1-sulfonamide
P6		4-amino-N-(4-methylpyrimidin-2-yl)benzene-1-sulfonamide
P7		2-hydroxy-5-[(1E)-2-{4-[(pyridin-2-yl)sulfamoyl]phenyl}diazen-1-yl]benzoic acid

Figure 1. Molecular structures, names, and abbreviations of studied inhibitors.

2.3. Monte Carlo Simulations

A 5 Å Fe (1 1 0) plate (surface unit cell (12 × 12)) was utilized to look at the adsorption setups of the studied molecules on mild steel. A permeable layer (30 Å thick vacuum layer) was added to the Fe (1 1 0) because it is the stable interface for iron. Then, to blend the sulfonamide in with 100 water molecules [17]. The COMPASS force field [18] was utilized to enhance the design of the entire system and to perform Monte Carlo reproductions utilizing the Studio 7.0 adsorption confinement module [19].

3. Results

3.1. Eco-Friendly Noxiousness and Solvency of Sulfonamide Derivative Inhibitors

The solvency and impacts of poisonousness are displayed in Table 1, where Log (IGC50) is the toxic effects of chemicals, determined by their concentration which gives half (50%) inhibitory development of species (typically in water). This kind of toxicity is normally estimated in simple water species, for example, Daphnia magna or Tetrahymena pyriformis [20]. Log P is like Log ($C_{octanol}/C_{water}$), where the positive Log P value shows the lipophilicity character of the examined molecule, and the negative value of this action demonstrates higher solvency of the examined molecule in the watery medium [21]. According to our in silico results, all Log P values on all wheels are negative, so one might say that these molecules have a decent dissolvability and great acridity. Table 1 shows that the IGC50 values are lower than the concentration used to control the corrosion of carbon steel in the watery medium. With these outcomes, these molecules can be ordered into eco-friendly materials [22].

Table 1. Predicted Log values (IGC50) and Log-P at the online chemical information site.

Inhibitors	Log (IGC50) in Log (mmol/L)	Log P in Log (mol/L)
P1	0.72	−3.0
P2	0.36	−3.1
P3	0.62	−3.7
P4	0.59	−2.6
P5	0.61	−2.4
P6	0.54	−2.5
P7	0.24	−1.4

3.2. Quantum Chemical Calculations (Evaluative Study)

Quantum theoretical calculations help to explore the electronic structure of molecules and provide a better understanding of the correlation between the molecular properties and their subsequent inhibition capability [23]. Frontier molecular orbital energies affect the inhibitor molecules' adsorption to the metallic surface. The lowest and highest occupied molecular orbital (LUMO and HOMO) define the electron-accepting and donating ability of molecules. E_{HOMO} frequently corresponds with the possible electron-donating properties of the inhibitor. A high E_{HOMO} value demonstrates a higher electron-donating ability of the inhibitor to the vacant d-orbital of the mild steel. However, the E_{LUMO} value corresponds with the possible electron-accepting properties of the inhibitor. The low value of E_{LUMO} builds the electron take-up capability of the inhibitory molecule by the filled Fe orbital. The energy gap ΔE is additionally used to portray the conduct of inhibitory adsorption molecules on metal surfaces. A decrease in the value of ΔE implies a decrease in the chemical reactivity of the inhibitor molecules which enhances the molecules' adsorption mechanism by the formation of a protective film [24,25]. According to the literature, if the fraction of electron transferred value is less than (3.6), the inhibitor electron-donating tendency is brought up [26,27]. Dipole moment is related to the molecule's charge distribution and polarity. A high dipole moment value demonstrates a large interaction between inhibitor molecules and the metal surface which leads to high inhibition efficiency [28]. The computed molecular parameters E_{HOMO}, E_{LUMO}, and dipole moment (μ), and the other calculated quantum chemical parameters were achieved for both aqueous (A) and gaseous (G) neutral forms of inhibitors and their corresponding values are given in Table 2.

3.2.1. Quantum Chemical Parameters

An inspection of Table 2 reveals that all the inhibitors present high dipole moment values which suggest that the sulfonamide molecules are polar, this allows bands to form and leads to better adherence to the metal surface [29], also, all the molecules have ΔN values in the average of 0.6 which explains the ability of this molecule to strongly interact with the metal surface. A molecule with a lower value of ΔE has higher reactivity and better adsorption to the steel surface, consequently, the inhibition efficiency order of the sulfonamide molecules is P7 > P5 > P6 > P1 > P2 > P3 > P4.

Table 2. Quantum chemical parameters for neutral sulfonamide molecules in the aqueous and gaseous phase.

Parameter	Phase	P1	P2	P3	P4	P5	P6	P7
E_{HOMO} (eV)	G	−6.3094	−6.1404	−6.3407	−6.2196	−6.2133	−6.1793	−6.3777
	A	−6.0871	−6.0672	−6.0794	−6.0710	−6.0612	−6.0547	−6.3758
E_{LUMO} (eV)	G	−1.0006	−0.7717	−0.9323	−0.7481	−0.8858	−0.8858	−2.7481
	A	−1.0896	−0.8874	−0.8651	−0.8245	−1.2711	−1.1794	−2.7555
ΔE_{gap} (eV)	G	5.3088	5.3687	5.4084	5.4715	5.3276	5.2936	3.6295
	A	4.9975	5.1798	5.2144	5.2465	4.7901	4.8753	3.6203
μ (D)	G	7.1957	4.6421	7.2462	8.3757	5.5911	4.8601	5.5137
	A	9.5700	6.4420	9.8034	12.3497	8.0687	7.1703	5.7823
η (eV)	G	2.6544	2.6843	2.7042	2.7358	2.6638	2.6468	1.8148
	A	2.4987	2.5899	2.6072	2.6232	2.3951	2.4377	1.8101
σ (eV^{-1})	G	0.3767	0.3725	0.3698	0.3655	0.3754	0.3778	0.5510
	A	0.4002	0.3861	0.3836	0.3812	0.4175	0.4102	0.5524
χ (eV)	G	3.6550	3.4561	3.6365	3.4838	3.5495	3.5325	4.5629
	A	3.5883	3.4773	3.4723	3.4478	3.6661	3.6170	4.5656
ΔN	G	0.6301	0.6601	0.6219	0.6426	0.6477	0.6550	0.6715
	A	0.6827	0.6801	0.6765	0.6771	0.6960	0.6939	0.6724
ω	G	2.5164	2.2248	2.4451	2.2182	2.3649	2.3573	5.7363
	A	2.5765	2.3344	2.3122	2.2657	2.8059	2.6835	5.7578
ε	G	0.3974	0.4495	0.4090	0.4508	0.4228	0.4242	0.1743
	A	0.3881	0.4284	0.4325	0.4414	0.3564	0.3726	0.1737

3.2.2. Optimized Structures and Density Distribution

Sulfonamides are the molecules that contain the $S(=O)_2–NH_2–)$ sulfonamide functional group. The electron density distribution of HOMO and LUMO is displayed in Figure 2, which shows the HOMO orbitals are for the NH_2 group and the phenyl ring of practically all neutral sulfa drugs. The LUMO extends over the SO_2 and into the NH_2 side-chain group which recommends that the inhibitor molecules could be adsorbed on the corroding metal surface through the protonated amine function in acidic corrosive media by creating bonds between the Fe (d-orbital) and the lone pairs of electrons (sp^2) existing on the oxygen and nitrogen atoms of both the heterocyclic rings and the sulfonamide group [30,31]. The molecular sizes of P1, P2, P3, and P4 sulfa drugs are relatively small compared to P5, P6, and P7. That may result in low surface coverage and consequently lead to a slight diminution in the inhibition effect of these compounds.

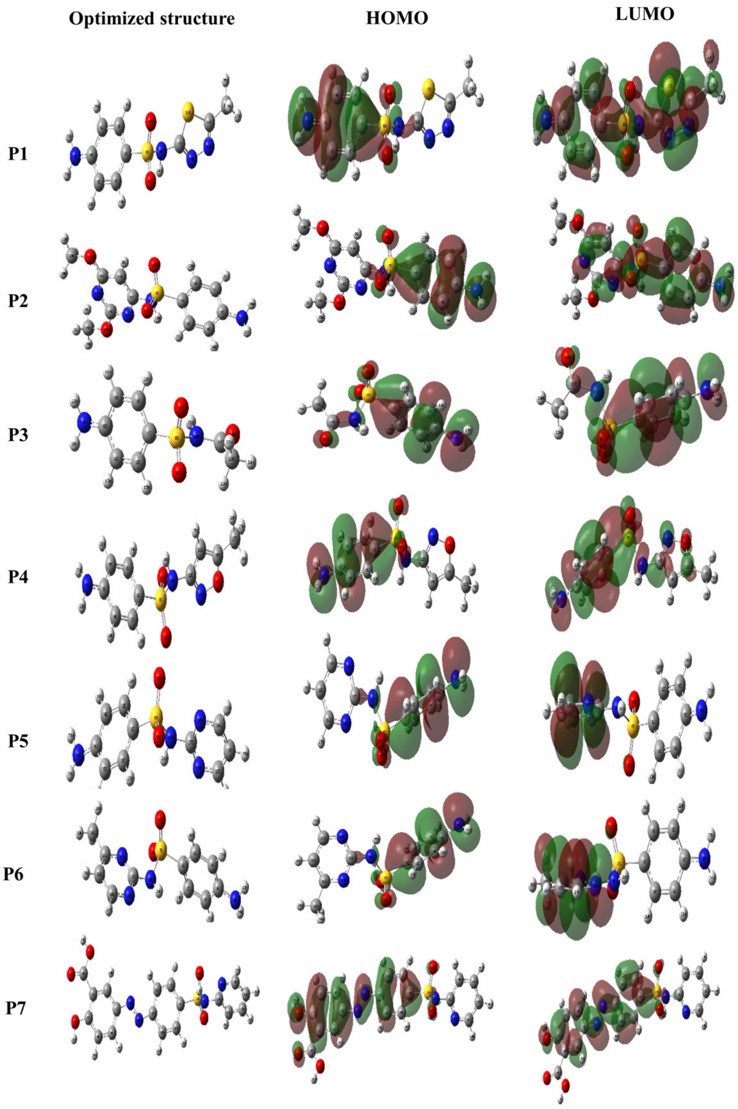

Figure 2. Optimized structures, the highest occupied molecular orbital (HOMO), and the lowest occupied molecular orbital (LUMO) energies of the studied sulfonamide molecules.

3.2.3. Fukui Functions

Fukui functions define the molecule's sites where nucleophilic, electrophilic, and radical attacks may occur. These local descriptors were calculated from natural populations for each atom in neutral, anionic, and cationic forms using the following equations:

$$f^0 = P_k(N+1) - P_k\ (N-1) \tag{6}$$

$$f_k^+ = P_k(N+1) - P_k\ (N\ ) \tag{7}$$

$$f_k^- = P_k(N) - P_k\ (N-1\ ) \tag{8}$$

where, $P_k(N)$, $P_k(N + 1)$, and $P_k(N - 1)$ are, respectively, the natural populations in the neutral, anionic, and cationic species for the atom k. Table 3 shows the Fukui functions of sulfonamide investigated inhibitors. We notice that the highest values of the electrophilic index f_k^+ are localized on the atoms C1, C4, C5, N7 for the molecules P1, P2, and P3, on the atoms C1, C4, N7 for the molecule P4 and P5, and on the atoms C1, C4, N8, N16, N17 for the molecule P6, and finally, on the atoms N11, N12 for the molecule P7. These sites could be electron acceptors. The electrophilicity's index f_k^- high values are shown on the atom S13 for the molecule P1, on the atom C12 for the molecule P2, on the atom C3 for the molecule P3, on the atom C4 for the molecule P4, on the atoms C13, C14, N15, N16 for the molecule P5, and on the atoms C14, C15 for the molecule P6, and finally, on the atoms N11 and N12 for the molecule P7. Consequently, these could donate electrons. The obtained results elucidate that the considered sulfa drugs may highly adsorb on the steel surface.

Table 3. Fukui functions of sulfonamide investigated inhibitors.

Molecules	**Atoms**	**P(N)**	**P(N + 1)**	**P(N − 1)**	f_k^+	f_k^-	f_k^0
P1	C1	−0.39000	−0.43077	−0.25203	0.13797	0.04077	0.17874
	C4	−0.27935	−0.32756	−0.16711	0.11224	0.04821	0.16045
	C5	−0.27637	−0.28465	−0.17584	0.10053	0.00828	0.10881
	N7	−0.86354	−0.89131	−0.56385	0.29969	0.02777	0.32746
	S13	0.62527	0.46206	0.63484	0.00957	0.16321	0.02777
P2	C1	−0.38341	−0.41526	−0.24402	0.13939	0.03185	0.17124
	C4	−0.27974	−0.33061	−0.16397	0.11577	0.05087	0.16664
	C5	−0.27662	−0.27662	−0.17605	0.10057	0.01162	0.11219
	N7	−0.86377	−0.86377	−0.55903	0.30474	0.02484	0.32958
	C12	0.42534	0.42534	0.42347	−0.00187	0.12431	0.12244
P3	C1	−0.38898	−0.45406	−0.24823	0.14075	0.06508	0.20583
	C3	−0.19837	−0.37833	−0.19383	0.00454	0.17996	0.18450
	C4	−0.27982	−0.37898	−0.16368	0.11614	0.09916	0.21530
	C5	−0.27649	−0.29821	−0.17523	0.10126	0.02172	0.12298
	N7	−0.86345	−0.90271	−0.55757	0.30588	0.03926	0.34514
P4	C1	−0.38787	−0.43648	−0.24895	0.13892	0.04861	0.18753
	C4	−0.28166	−0.44493	−0.16724	0.11442	0.16327	0.27769
	N7	−0.86593	−0.90138	−0.56718	0.29875	0.03545	0.33420
P5	C1	−0.38724	−0.38580	−0.24883	0.13841	−0.00144	0.13697
	C4	−0.28047	−0.28265	−0.28047	0.11461	0.00218	0.11679
	N7	−0.86496	−0.86840	−0.56459	0.30037	0.00344	0.30381
	C13	−0.05441	−0.16647	−0.05736	0.00295	0.22088	0.22383
	C14	−0.05758	−0.15882	0.06082	0.00324	0.21640	0.21964
	N15	−0.52983	−0.67461	−0.52361	0.00622	0.14478	0.15100
	N16	−0.52678	−0.67355	−0.52617	0.00061	0.14677	0.14738
P6	C1	−0.38602	−0.38569	−0.24778	0.13824	−0.00033	0.13791
	C4	−0.28116	−0.28360	−0.16636	0.11480	0.00244	0.11724
	N8	−0.86527	−0.86931	−0.56615	0.29912	0.00404	0.30316
	C14	0.05800	−0.16854	0.06084	0.00284	0.22654	0.22938
	C15	0.26740	0.08589	0.27070	0.00330	0.18151	0.18481
	N16	−0.66657	−0.54195	−0.53561	0.13096	−0.12462	0.00634
	N17	−0.68583	−0.53278	−0.53267	0.15316	−0.15305	0.00011
P7	N11	−0.17714	−0.35222	−0.17714	0.19310	0.17508	0.361818
	N12	−0.21169	−0.35404	−0.21169	0.19792	0.14235	0.34027

3.2.4. MCS Results

Monte Carlo simulation is a great method to explain the adsorption behavior of inhibitors onto the surface of metals [32]. We have investigated the MCS of the tested molecules on the iron surface. The stable configuration related to the low adsorption energy value of the examined inhibitors P1, P2, P3, P4, P5, P6, and P7 molecules onto the surface of iron is represented in Figure 3.

Table 4 shows the MC simulation parameters for all the studied molecules. As a rule, the mechanism of protection of metal corrosion inhibitors is through the adsorption process [33]. In this way, adsorption energy values can be a viable aspect for first-class inhibitors [34]. The higher the negative adsorption energy proportion, the more steady and solid the adsorption arrangement [35]. The energy values P1, P2, P3, P4, P5, P6, and P7 were obtained by this simulation. Performance for the adsorption of the studied sulfonamide derivatives on the outer layer of Fe (110) happens as follows: P7 > P5 > P6 > P1 > P2 > P3 > P4. This series matches with the series obtained by the DFT technique. Each inhibitor examined was adsorbed at a parallel position on the Fe surface (110) to maximize the contact surface and shield the carbon steel from the corrosion process [36]. The outcomes show that the adsorption energy of the investigated molecules is higher than that of the water molecules. This shows the capacity of water molecules on the outer layer of the carbon steel surface with the arrangement of a steady layer that can protect the carbon steel from corrosion in the aqueous corrosive media [37,38].

Table 4. MC simulation parameters (in kcal/mol).

Systems	Adsorption Energy Inhibitors	Adsorption Energy Water
Fe(110)/P1/100H_2O	−1692.52	−16.92
Fe(110)/P2/100H_2O	−1694.91	−12.71
Fe(110)/P3/100H_2O	−1693.98	−13.71
Fe(110)/P4/100H_2O	−1711.78	−14.11
Fe(110)/P5/100H_2O	−1719.78	−10.97
Fe(110)/P6/100H_2O	−1698.35	−13.62
Fe(110)/P7/100H_2O	−1719.79	−16.43

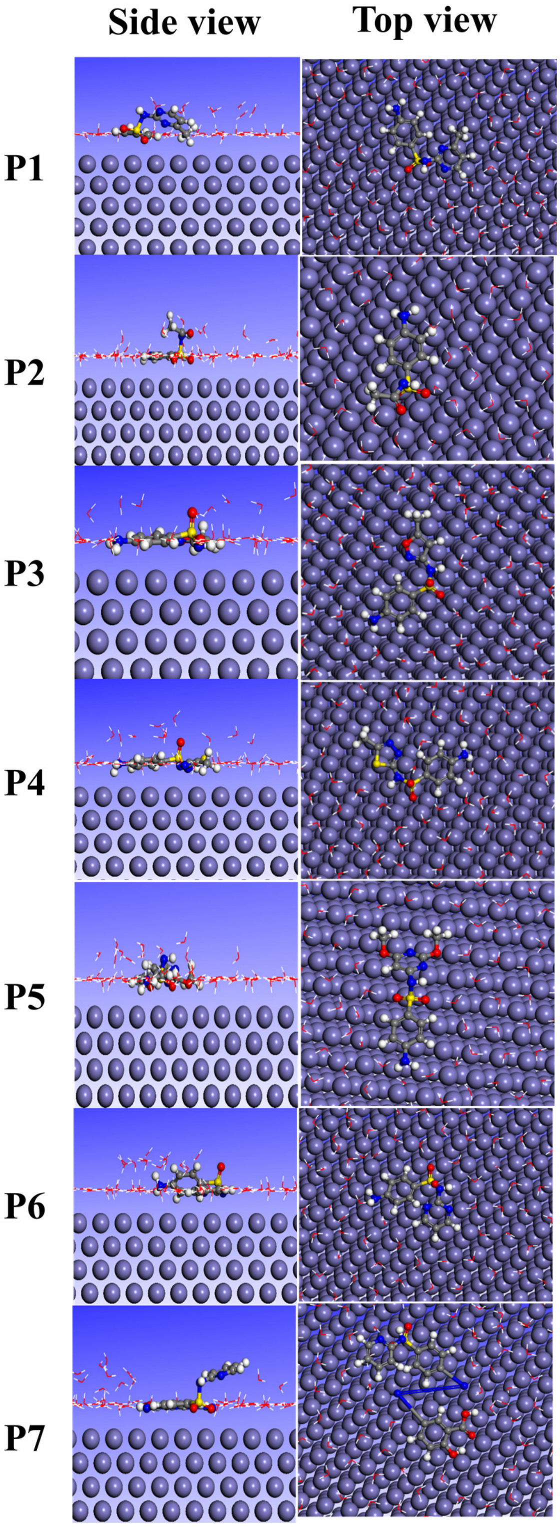

Figure 3. The stable configuration related to the low adsorption energy value of examined inhibitors P1, P2, P3, P4, P5, P6, and P7 molecules onto the surface of the iron.

4. Inhibition Mechanism of NAR1

From the computational results of the sulfonamide inhibitors, the most probable mechanism of adsorption of P7 can be described as shown in Figure 4. The P7 inhibitor could be adsorbed on the mild steel by various interaction types. A chemical interaction (chemisorption) can occur with the vacant d-orbital of Fe, such as the interaction with the oxygen, sulfur, and nitrogen atoms with the steel surface by sharing their lone-pair electrons which make a strong bond that can protect the mild steel from the corrosion process. In addition, a retro-donation interaction was shown between the ionized Fe atoms on the surface and the π- electron of the aromatic ring. Furthermore, the parallel adsorption of the P7 covered a large surface area explaining the formation of a protective film over the steel surface and thus a higher inhibition performance.

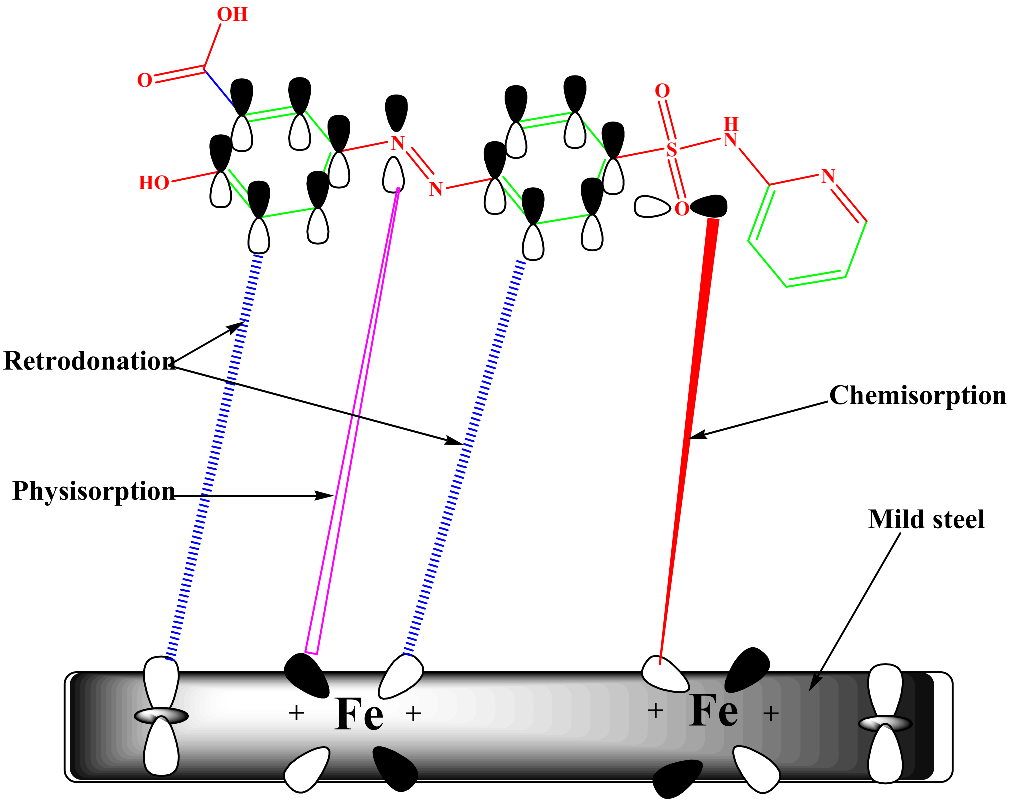

Figure 4. Proposed inhibition mechanism of P7.

5. Conclusions

Relating to the in silico toxicity tests, the investigated inhibitors can be classified as eco-friendly products. Theoretical density functional calculations and molecular Monte Carlo simulations both confirm that the examined sulfa drug compounds might be considered efficient as corrosion inhibitors in the aqueous medium. Fukui functions results confirm that the studied inhibitors can share electrons with the iron's vacant orbital via hetero atoms (likely nitrogen, sulfur, and oxygen) and π electrons. The order of the inhibition efficiency predictive order shown by DFT at B3LYP and Monte Carlo simulation is P7 > P5 > P6 > P1 > P2 > P3 > P4.

This study motivates researchers to develop and synthesize sulfonamide inhibitors and test their efficiency in a different interface.

Author Contributions: S.A.M.: writing—original draft, conceptualization, investigation, visualization. N.A.: methodology, validation. R.H.; writing—original draft, conceptualization, investigation visualization (equal contribution). A.A.L.: reviewing and editing paper. A.A.: methodology, software, validation. T.S.: reviewing and editing paper. M.T.: conceptualization, visualization. S.-C.K.: conceptualization, investigation visualization. All authors have read and agreed to the published version of the manuscript.

Funding: This research received no external funding.

Conflicts of Interest: The authors declare no conflict of interest.

References

1. Haldhar, R.; Prasad, D.; Saxena, A.; Singh, P. Valeriana wallichii root extract as a green & sustainable corrosion inhibitor for mild steel in acidic environments: Experimental and theoretical study. *Mater. Chem. Front.* **2018**, *2*, 1225–1237. [CrossRef]
2. Haldhar, R.; Prasad, D.; Bahadur, I.; Dagdag, O.; Kaya, S.; Verma, D.K.; Kim, S.-C. Investigation of plant waste as a renewable biomass source to develop efficient, economical and eco-friendly corrosion inhibitor. *J. Mol. Liq.* **2021**, *335*, 116184. [CrossRef]
3. Yadav, D.K.; Quraishi, M.A. Electrochemical investigation of Substituted Pyranopyrazoles Adsorption on Mild Steel in Acid Solution. *Ind. Eng. Chem. Res.* **2012**, *51*, 8194–8210. [CrossRef]
4. Bouoidina, A.; Ech-Chihbi, E.; El-Hajjaji, F.; El Ibrahimi, B.; Kaya, S.; Taleb, M. Anisole derivatives as sustainable-green inhibitors for mild steel corrosion in 1 M HCl: DFT and molecular dynamic simulations approach. *J. Mol. Liq.* **2020**, *324*, 115088. [CrossRef]
5. Haldhar, R.; Prasad, D.; Saxena, A.; Kumar, R. Experimental and theoretical studies of Ficus religiosa as green corrosion inhibitor for mild steel in 0.5 M H_2SO_4 solution. *Sustain. Chem. Pharm.* **2018**, *9*, 95–105. [CrossRef]
6. Haldhar, R.; Prasad, D.; Saxena, A. Armoracia rusticana as sustainable and eco-friendly corrosion inhibitor for mild steel in 0.5M sulphuric acid: Experimental and theoretical investigations. *J. Environ. Chem. Eng.* **2018**, *6*, 5230–5238. [CrossRef]
7. Markhali, B.P.; Naderi, R.; Mahdavian, M.; Sayebani, M.; Arman, S.Y. Electrochemical impedance spectroscopy and electrochemical noise measurements as tools to evaluate corrosion inhibition of azole compounds on stainless steel in acidic media. *Corros. Sci.* **2017**, *75*, 269–279. [CrossRef]
8. Haldhar, R.; Prasad, D.; Bahadur, I.; Dagdag, O.; Berisha, A. Evaluation of Gloriosa superba seeds extract as corrosion inhibition for low carbon steel in sulfuric acidic medium: A combined experimental and computational studies. *J. Mol. Liq.* **2020**, *323*, 114958. [CrossRef]
9. Haldhar, R.; Prasad, D.; Saxena, A.; Kaur, A. Corrosion resistance of mild steel in 0.5 M H_2SO_4 solution by plant extract of Alkana tinctoria: Experimental and theoretical studies. *Eur. Phys. J. Plus* **2018**, *133*, 356. [CrossRef]
10. Tan, B.; Zhang, S.; Cao, X.; Fu, A.; Guo, L.; Marzouki, R.; Li, W. Insight into the anti-corrosion performance of two food flavors as eco-friendly and ultra-high performance inhibitors for copper in sulfuric acid medium. *J. Colloid Interface Sci.* **2021**, *609*, 838–851. [CrossRef]
11. Nahle, A.; Salim, R.; El Hajjaji, F.; Aouad, M.R.; Messali, M.; Ech-chihbi, E.; Hammoutid, B.; Taleb, M. Novel triazole deriva-tives as ecological corrosion inhibitors for mild steel in 1.0 M HCl: Experimental & theoretical approach. *RSC Adv.* **2021**, *11*, 4147.
12. Leeson, P.D.; SpringThorpe, B. Classification of a diverse set of Tetrahymena pyriformis toxicity chemical compounds from molecular descriptors by statistical learning methods. *Nat. Rev. Drug Discov.* **2007**, *6*, 881–890. [CrossRef] [PubMed]
13. Xue, Y.; Li, Z.R.; Yap, C.W.; Sun, L.Z.; Chen, A.X.; Chen, Y.Z. Effect of Molecular Descriptor Feature Selection in Support Vector Machine Classification of Pharmacokinetic and Toxicological Properties of Chemical Agents. *J. Chem. Inf. Comput. Sci.* **2004**, *44*, 1630–1638. [CrossRef] [PubMed]
14. Guo, L.; Tan, J.; Kaya, S.; Leng, S.; Li, Q.; Zhang, F. Multidimensional insights into the corrosion inhibition of 3,3-dithiodipropionic acid on Q235 steel in H_2SO_4 medium: A combined experimental and in silico investigation. *J. Colloid Interface Sci.* **2020**, *570*, 116–124. [CrossRef] [PubMed]
15. Yadav, M.; Behera, D.; Kumar, S. Experimental and theoretical investigation on adsorption and corrosion inhibition properties of imidazopyridine derivatives on mild steel in hydrochloric acid solution. *Surf. Interface Anal.* **2014**, *46*, 640–652. [CrossRef]
16. Karakus, N.; Sayin, K. The investigation of corrosion inhibition efficiency on some benzaldehyde thiosemicarbazones and their thiole tautomers: Computational study. *J. Taiwan Inst. Chem. Eng.* **2015**, *48*, 95–102. [CrossRef]
17. El Hajjaji, F.; Abrigach, F.; Hamed, O.; Hasan, A.R.; Taleb, M.; Jodeh, S.; Rodríguez-Castellón, E.; Yuso, M.D.V.M.D.; Algarra, M. Corrosion Resistance of Mild Steel Coated with Orgainc Material Containing Pyrazol Moiety. *Coatings* **2018**, *8*, 330. [CrossRef]
18. Arrousse, N.; Salim, R.; Al Houari, G.; El Hajjaji, F.; Zarrouk, A.; Rais, Z.; Taleb, M.; Chauhan, D.S.; Quraishi, M.A. Experimental and theoretical insights on the adsorption and inhibition mechanism of (2E)-2-(acetylamino)-3-(4-nitrophenyl) prop-2-enoic acid and 4-nitrobenzaldehyde on mild steel corrosion. *J. Chem. Sci.* **2020**, *132*, 112. [CrossRef]
19. Ellison, C.; Cronin, M.; Madden, J.; Schultz, T. Experimental Reactivity Parameters for Toxicity Modeling: Application to the Acute Aquatic Toxicity of SN2 Electrophiles to *Tetrahymena pyriformis*. *SAR QSAR Environ. Res.* **2008**, *19*, 751–783. [CrossRef]
20. Chang, L.C.; Spanjersberg, R.F.; Künzel, J.K.V.D.; Mulder-Krieger, T.; van den Hout, G.; Beukers, J.M.W.; Ijzerman, A.P. Browsing JRC QSAR Model Database. Available online: https://qsardb.org/repository/handle/10967/109 (accessed on 1 February 2022).
21. Tantawy, A.H.; Soliman, K.A.; El-Lateef, H.M.A. Experimental and computational approaches of sustainable quaternary bisammonium fluorosurfactants for corrosion inhibition as protective films at mild steel/H_2SO_4 interface. *Colloids Surf. A Physicochem. Eng. Asp.* **2021**, *614*, 126141. [CrossRef]
22. Verma, C.; Quraishi, M.A.; Singh, A. 5-substituted 1H-tetrazoles as effective corrosion inhibitors for mild steel in 1M hydro-chloric acid. *J. Taibah Univ. Sci.* **2016**, *10*, 718–733. [CrossRef]
23. Haldhar, R.; Prasad, D.; Mandal, N.; Benhiba, F.; Bahadur, I.; Dagdag, O. Anticorrosive properties of a green and sustainable inhibitor from leaves extract of Cannabis sativa plant: Experimental and theoretical approach. *Colloids Surf. A Physicochem. Eng. Asp.* **2021**, *614*, 126211. [CrossRef]
24. Arrousse, N.; Salim, R.; Kaddouri, Y.; Zarrouk, A.; Zahri, D.; El Hajjaji, F.; Touzani, R.; Taleb, M.; Jodeh, S. The inhibi-tion behavior of Two pyrimidine-pyrazole derivatives against corrosion in hydrochloric solution: Experimental, surface analysis and in silico approach studies. *Arab. J. Chem.* **2020**, *13*, 5949–5965. [CrossRef]

25. Haldhar, R.; Prasad, D.; Kamboj, D.; Kaya, S.; Dagdag, O.; Guo, L. Corrosion inhibition, surface adsorption and computational studies of Momordica charantia extract: A sustainable and green approach. *SN Appl. Sci.* **2021**, *3*, 25. [CrossRef]
26. El-Hajjaji, F.; Messali, M.; de Yuso, M.V.M.; Rodríguez-Castellón, E.; Almutairi, S.; Bandosz, T.J.; Algarra, M. Effect of 1-(3-phenoxypropyl) pyridazin-1-ium bromide on steel corrosion inhibition in acidic medium. *J. Colloid Interface Sci.* **2019**, *541*, 418–424. [CrossRef]
27. Mrani, S.A.; El Arrouji, S.; Karrouchi, K.; El Hajjaji, F.; Alaoui, K.I.; Rais, Z.; Taleb, M. Inhibitory performance of some Pyrazole derivatives against corrosion of mild steel in 1.0 M HCl: Electrochemical, MEB and theoretical studies. *Int. J. Corros. Scale Inhib.* **2018**, *7*, 542–569.
28. Arrousse, N.; Mabrouk, E.; Hammouti, B.; El hajjaji, F.; Rais, Z.; Taleb, M. Synthesis, characterization, anti-corrosion behavior and theoretical study of the new organic dye: 3- oxo-3Hspiro[isobenzofuran-1,9′-xanthene]-3´,6´-diyl bis(3-methylbenzenesulfonate). *Int. J. Corros. Scale Inhib.* **2020**, *9*, 661–687.
29. El-Hajjaji, F.; Ech-Chihbi, E.; Rezki, N.; Benhiba, F.; Taleb, M.; Chauhan, D.S.; Quraishi, M. Electrochemical and theoretical insights on the adsorption and corrosion inhibition of novel pyridinium-derived ionic liquids for mild steel in 1 M HCl. *J. Mol. Liq.* **2020**, *314*, 113737. [CrossRef]
30. Ouakki, M.; Galai, M.; Rbaa, M.; Abousalem, A.S.; Lakhrissi, B.; Touhami, M.E.; Cherkaoui, M. Electrochemical, thermody-namic and theoretical studies of some imidazole derivatives compounds as acid corrosion inhibitors for mild steel. *J. Mol. Liq.* **2020**, *319*, 114063. [CrossRef]
31. Shariatinia, Z.; Ahmadi-Ashtiani, A. Corrosion inhibition efficiency of some phosphoramide derivatives: DFT computations and MD simulations. *J. Mol. Liq.* **2019**, *292*, 111409. [CrossRef]
32. Ghazoui, A.; Benchat, N.; El-Hajjaji, F.; Taleb, M.; Rais, Z.; Saddik, R.; Elaatiaoui, A.; Hammouti, B. The study of the effect of ethyl (6-methyl-3-oxopyridazin-2-yl) acetate on mild steel corrosion in 1M HCl. *J. Alloys Compd.* **2017**, *693*, 510–517. [CrossRef]
33. Tan, B.; Zhang, S.; Liu, H.; Guo, Y.; Qiang, Y.; Li, W.; Guo, L.; Xu, C.; Chen, S. Corrosion inhibition of X65 steel in sulfuric acid by two food flavorants 2-isobutylthiazole and 1-(1,3-Thiazol-2-yl) ethanone as the green environmental corrosion inhibitors: Combination of experimental and theoretical researches. *J. Colloid Interface Sci.* **2018**, *538*, 519–529. [CrossRef] [PubMed]
34. Haldhar, R.; Prasad, D.; Saxena, A. Myristica fragrans extract as an eco-friendly corrosion inhibitor for mild steel in 0.5M H2SO4 solution. *J. Environ. Chem. Eng.* **2018**, *6*, 2290–2301. [CrossRef]
35. Haldhar, R.; Kim, S.-C.; Prasad, D.; Bedair, M.; Bahadur, I.; Kaya, S.; Dagdag, O.; Guo, L. Papaver somniferum as an efficient corrosion inhibitor for iron alloy in acidic condition: DFT, MC simulation, LCMS and electrochemical studies. *J. Mol. Struct.* **2021**, *1242*, 130822. [CrossRef]
36. Haldhar, R.; Prasad, D.; Nguyen, L.T.; Kaya, S.; Bahadur, I.; Dagdag, O.; Kim, S.-C. Corrosion inhibition, surface adsorption and computational studies of Swertia chirata extract: A sustainable and green approach. *Mater. Chem. Phys.* **2021**, *267*, 124613. [CrossRef]
37. Arrousse, N.; Mabrouk, E.; Salim, R.; Alaoui, K.I.; El Hajjaji, F.; Rais, Z.; Taleb, M.; Hammouti, B. Fluorescein as commercial and environmentally friendly inhibitor against corrosion of mild steel in molar hydrochloric acid medium. *Mater. Today Proc.* **2020**, *27*, 3184–3192. [CrossRef]
38. Haldhar, R.; Prasad, D.; Bhardwaj, N. Surface adsorption and corrosion resistance performance of Acacia concinna pod extract: An efficient inhibitor for mild steel in acidic environment. *Arab. J. Sci. Eng.* **2020**, *45*, 131–141. [CrossRef]